

# Unified Coupled-Channels and Hauser-Feshbach Model Calculation for Nuclear Data Evaluation

Toshihiko Kawano

Los Alamos National Laboratory, Los Alamos, NM 87545, USA

Email: kawano@lanl.gov

We present an overview of the coupled-channels optical model and the Hauser-Feshbach theory code CoH<sub>3</sub>, which focuses on the nuclear reaction calculations in the keV to tens of MeV region with special attention to the nuclear deformation. The code consists of three major sections that undertake the one-body potential mean-field theory, the coupled-channels optical model, and the Hauser-Feshbach statistical decay. There are other complementary segments to perform the whole nuclear reaction calculations, such as the direct/semidirect radiative capture process, pre-equilibrium process, and prompt fission neutron emission.

## 1. Introduction

Modern methodology for evaluating nuclear reaction data for medium to heavy mass targets centers a statistical Hauser-Feshbach (HF) code in the evaluation system. The HF theory with the width fluctuation correction gives a compound nuclear reaction cross section when resonances are strongly overlapped; in other words, an energy-averaged cross section is calculated. The HF codes currently available in the market, such as EMPIRE [1], TALYS [2], CCONE [3], and CoH<sub>3</sub> [4], which are capable for multi-particle evaporation from a compound nucleus, provide complete information of nuclear reactions, not only the reaction cross sections, but also the energy and angular distributions of secondary particles,  $\gamma$ -ray production cross sections, isomeric state productions, and so on. One of distinct features in CoH<sub>3</sub> is a unique capability to combine the coupled-channels optical model and the HF theory, where two methods are employed — the generalized transmission coefficients [5] and the Engelbrecht-Weidenmüller transformation [6]. Recently a code comparison was performed amongst the developers of EMPIRE, TALYS, CCONE, and CoH<sub>3</sub>, which suggested that the inelastic scattering cross section by CoH<sub>3</sub> tends to be slightly higher than the other codes [7] due to this difference. This paper outlines the reaction theories involved in CoH<sub>3</sub>.

## 2. CoH<sub>3</sub> Code Overview

The CoH<sub>3</sub> code is written in C++, and it consists of about 200 source files including 80 defined classes. For example, the simplest class is `ZAnumber` that has only two private member variables, the  $Z$  and  $A$  numbers. This class facilitates to calculate the  $(Z, A)$  pair of a compound nucleus

emerging in a reaction chain, and it resembles the traditional technique to represent the  $(Z, A)$  pair by an index of  $1000Z + A$  in the FORTRAN77-age.

CoH<sub>3</sub> has its own optical model solver to generate the transmission coefficients internally. In the deformed nucleus case, a rotational or vibrational model is employed for the coupled-channels (CC) calculation. The nuclear structure properties are determined by reading the nuclear structure database [8]. At higher excitation energies, we use the Gilbert-Cameron level density formula [9] with updated parameters [10]. CoH<sub>3</sub> allows overlapping discrete levels inside the continuum region. The width fluctuation correction is calculated by applying the method of Moldauer [11] with the LANL updated parameters [12] based on GOE (Gaussian Orthogonal Ensemble) [13]. When strongly coupled channels exist, the so-called Engelbrecht-Weidenmüller transformation (EWT) is invoked to diagonalize the  $S$ -matrix [6], and the width fluctuation is calculated in the diagonalized channel (eigen-channel) space.

Besides the main HF core part, the code consists of many models. The two-component exciton model [14, 15] is used to calculate the pre-equilibrium process. For fissioning nuclei, the prompt fission neutron spectrum is calculated with the Madland-Nix model [16] including pre-fission neutron emissions. The direct/semidirect (DSD) neutron capture process is calculated with the DSD model [17]. There are three mean-field theories included to calculate the single-particle wave-functions in a one-body potential; FRDM (Finite Range Droplet Model) [18, 19], HF-BCS (Hartree-Fock BCS) [17], and a simple spherical Woods-Saxon.

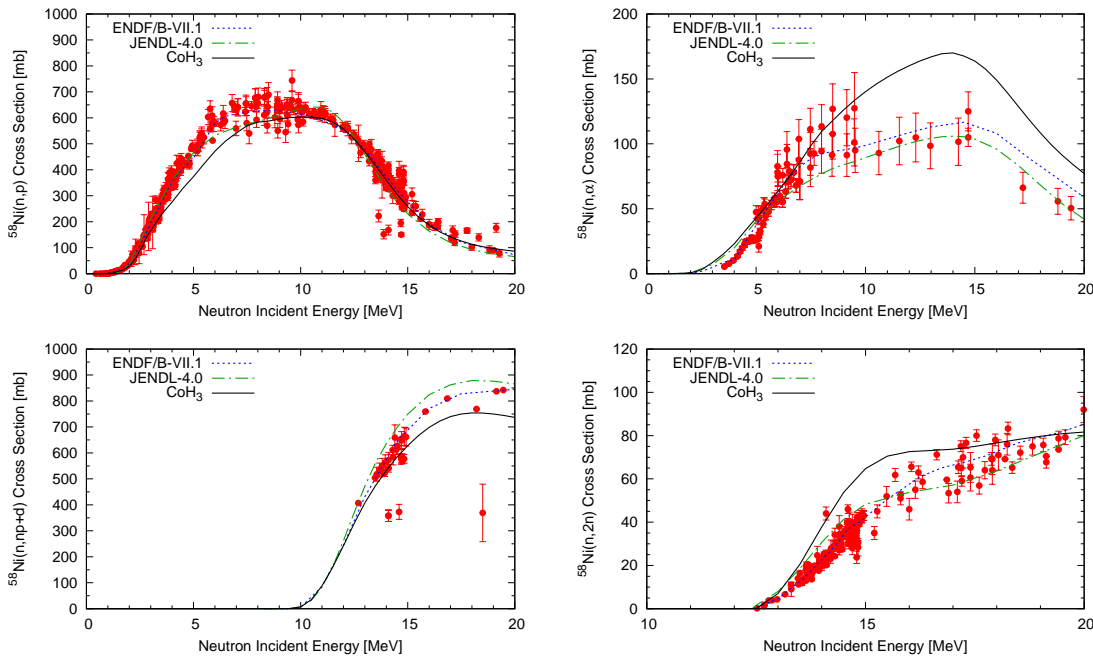


Fig. 1: CoH<sub>3</sub> default calculations for the neutron-induced reactions on <sup>58</sup>Ni; (n,p), (n,α), (n,np), and (n,2n) reactions. The (n,np) cross section includes the (n,d) reaction too.

Figure 1 demonstrates some default calculations of neutron-induced reactions on <sup>58</sup>Ni, comparing with the evaluated data in ENDF/B-VII.1 and JENDL-4.0, as well as experimental data

in literature (for the sake of simplicity, we use the same symbol for all available experimental data points.) These are relatively well behaved cases, and we suppose the other HF codes provide similar predictions. CoH<sub>3</sub> also produces the emitted particle angular distributions, which are shown in Fig. 2. The left panel shows the neutron elastic scattering that includes both the shape and compound elastic scattering cross sections, and the inelastic scattering to the first, second and third excited states of <sup>58</sup>Ni. The center panel is for the proton and the right is the  $\alpha$ -particle. The scattering angular distribution in a compound reaction process  $a + A \rightarrow b + B$  is calculated with the Blatt-Biedenharn formalism [20],

$$\left(\frac{d\sigma}{d\Omega}\right)_{ab} = \sum_L B_L P_L(\cos\theta_b) , \quad (1)$$

The  $B_L$  coefficient is given by Moldauer's statistical theory as

$$B_L = \frac{1}{4k^2} \frac{(-)^{I_B - I_A + s_b - s_a}}{(2s_a + 1)(2I_A + 1)} \sum_J (2J + 1)^2 \frac{1}{N_J} \\ \times \sum_{l_a j_a} \sum_{l_b j_b} W_{ab} \{X_{l_a j_a}(E_a) X_{l_b j_b}(E_b) + \delta_{I_A I_B} \delta_{E_a E_b} Y_{l_a j_a, l_b j_b}(E_a, E_b)\} , \quad (2)$$

where  $k$  is the incident particle wave number,  $W_{ab}$  is the width fluctuation correction factor,  $I$  and  $s$  are the spin of nucleus and particles, and

$$X_{lj}(E) = Z(ljlj; sL) W(jJjJ; lL) T_{lj}(E) , \quad (3) \\ Y_{l_a j_a, l_b j_b}(E_a, E_b) = (1 - \delta_{l_a l_b})(1 - \delta_{j_a j_b}) \{Z(l_a j_a l_b j_b; s_a L) W(J j_a J j_b; I_A L)\}^2 \\ \times T_{l_a j_a}(E_a) T_{l_b j_b}(E_b) , \quad (4)$$

where  $T_{lj}$  is the transmission coefficient,  $Z$  is the  $Z$ -coefficients, and the normalization  $N_J$  is given by integrating and summing all possible decay channels from the compound state  $J$ ,

$$N_J = \sum \int T_{lj}(E) dE. \quad (5)$$

For the Hauser-Feshbach theory,  $W_{ab} = 1$  and  $Y_{l_a j_a, l_b j_b}(E_a, E_b) = 0$ . In Fig. 2 case, the  $\alpha$ -particle emission that leaves the residual nucleus in its ground state, the  $(n, \alpha_0)$  reaction, shows large anisotropy [21].

### 3. Diagonalization of Coupled-Channels $S$ -Matrix

When strongly coupled channels exist, such as the direct inelastic scattering to the collective states, the scattering  $S$ -matrix contains some off-diagonal elements, hence we cannot apply the standard HF formalism. In CoH<sub>3</sub>, the coupled-channels  $S$ -matrix is transferred into the diagonalized eigen-channel space (EWT). Since Satchler's penetration matrix

$$P_{ab} = \delta_{ab} - \sum_c \langle S_{ac} \rangle \langle S_{bc}^* \rangle , \quad (6)$$

is Hermitian, this can be diagonalized by a unitary transformation [22]

$$(UPU^\dagger)_{\alpha\beta} = \delta_{\alpha\beta} p_\alpha , \quad 0 \leq p_\alpha \leq 1 , \quad (7)$$

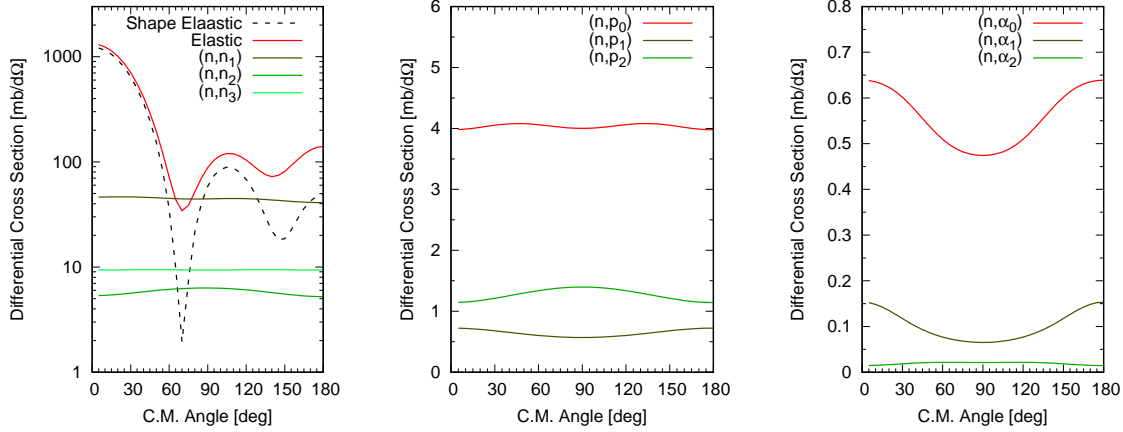


Fig. 2: Calculated secondary particle angular distributions for the neutron-induced reactions on  $^{58}\text{Ni}$  at  $E_n = 3$  MeV; neutron (left), proton (center), and  $\alpha$ -particle (right).

and the same matrix  $U$  diagonalizes the scattering matrix,

$$\langle \tilde{S} \rangle = U \langle S \rangle U^T . \quad (8)$$

Here the Roman letters are for the channel index in the physical space, and the Greek letters are for the eigen-channel. The width fluctuation correction is performed in the eigen-channel, and they are transformed back to the physical space

$$\sigma_{ab} = \sum_{\alpha\beta\gamma\delta} U_{\alpha a}^* U_{\beta b}^* U_{\gamma a} U_{\delta b} \langle \tilde{S}_{\alpha\beta} \tilde{S}_{\gamma\delta}^* \rangle , \quad (9)$$

where  $\langle \tilde{S}_{\alpha\beta} \tilde{S}_{\gamma\delta}^* \rangle$  is the width fluctuation corrected cross section in the eigen-channel. Rewriting Eq. (9) into more convenient form includes a term  $\langle \tilde{S}_{\alpha\alpha} \tilde{S}_{\beta\beta}^* \rangle$ , and we estimated this average by applying the GOE technique [6].

This transformation is still optional, since it requires longer computational time when the number of coupled-channels is large. When the transformation is not activated, CoH<sub>3</sub> calculates the generalized transmission coefficients from the coupled-channels  $S$ -matrix, where the direct reaction components are eliminated from the compound formation cross section [5], and a usual HF calculation is performed. This approximation works well when the target nucleus is not so strongly deformed. Figure 3 shows comparisons of the calculated elastic and inelastic scattering cross sections for the strongly deformed  $^{182}\text{W}$ , and two cases are given; the EWT case (solid curves) and the generalized transmission coefficients (dashed curves). A relatively large difference is seen in the first excited state case.

## 4. Conclusion

We outlined the coupled-channels Hauser-Feshbach code, CoH<sub>3</sub>. The code includes several models that are indispensable for producing evaluated nuclear data in the keV to tens of MeV region. The code is designed to fully utilize the coupled-channels calculation, which is especially

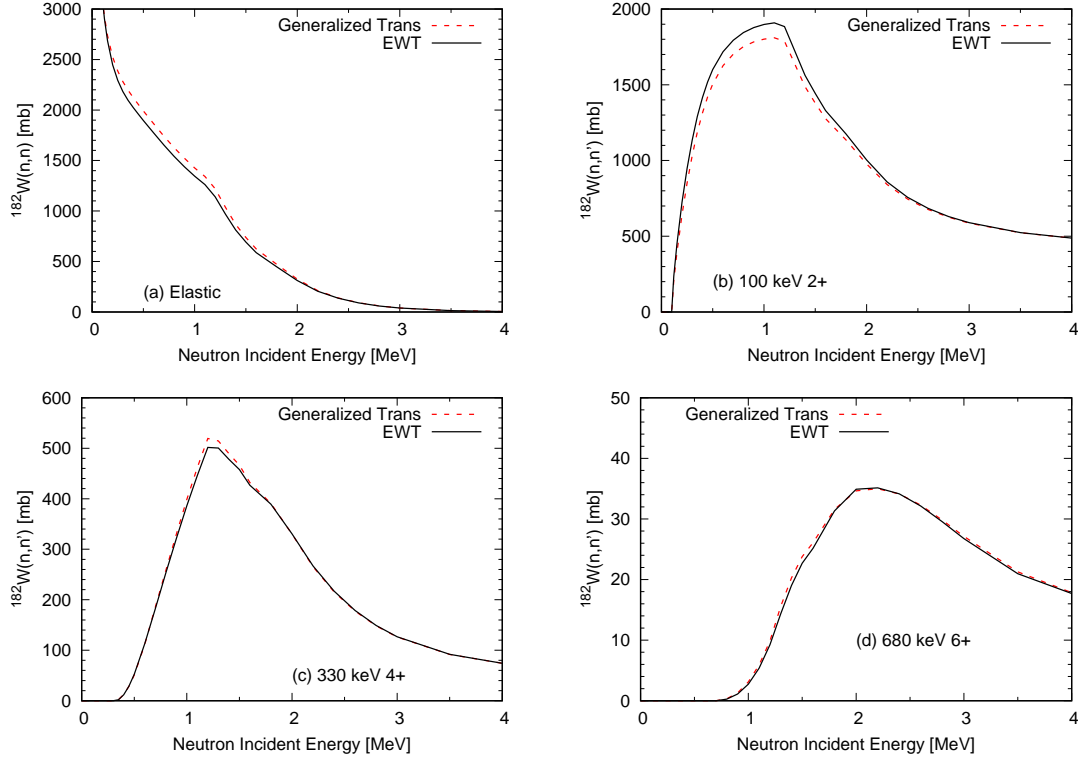


Fig. 3: Comparisons of the calculated (a) elastic and (b) – (d) inelastic scattering cross sections for  $^{182}\text{W}$ . The solid curves are the full Engelbrecht-Weidenmüller transformation (EWT) case, while the dashed curves are for the generalized transmission coefficient case.

important for evaluating nuclear data of deformed nuclei such as actinides. As an example, calculations for the neutron-induced elastic and inelastic scattering on  $^{182}\text{W}$  were shown, where two methods implemented in CoH<sub>3</sub> to combine the coupled-channels and the Hauser-Feshbach theories are employed.

## Acknowledgment

This work was carried out under the auspices of the National Nuclear Security Administration of the U.S. Department of Energy at Los Alamos National Laboratory under Contract No. 89233218CNA000001.

## References

- [1] M. Herman, *et al.*, INDC(NDS)-0603, International Atomic Energy Agency (2013).
- [2] A. J. Koning, S. Hilaire, and M. C. Duijvestijn, EPJ Web of Conferences, pages 211 – 214, (2008), Proc. Int. Conf. on Nuclear Data for Science and Technology, 22 – 27 Apr., 2007, Nice, France, Ed. O. Bersillon, F. Gunsing, E. Bauge, R. Jacqmin, and S. Leray.
- [3] O. Iwamoto, J. Nucl. Sci. Technol., **44**, 687 (2007).

- [4] T. Kawano, P. Talou, M. B. Chadwick, and T. Watanabe, *J. Nucl. Sci. Technol.*, **47**, 462 (2010).
- [5] T. Kawano, P. Talou, J. E. Lynn, M. B. Chadwick, and D. G. Madland, *Phys. Rev. C*, **80**, 024611 (2009).
- [6] T. Kawano, R. Capote, S. Hilaire, and P. Chau Huu-Tai, *Phys. Rev. C*, **94**, 014612 (2016).
- [7] R. Capote, S. Hilaire, O. Iwamoto, T. Kawano, and M. Sin, *EPJ Web Conf.*, **146**, 12034 (2017), ND 2016: Proc. Int. Conf. Nuclear Data for Science and Technology, Bruges, Belgium, September 11 - 16, 2016, A. Plompen, F.-J. Hamsch, P. Schillebeeckx, W. Mondelaers, J. Heyse, S. Kopecky, P. Siegler and S. Oberstedt (Eds.).
- [8] R. Capote, *et al.*, *Nuclear Data Sheets*, **110**, 3107 (2009).
- [9] A. Gilbert and A.G.W. Cameron, *Can. J. Phys.*, **43**, 1446 (1965).
- [10] T. Kawano, S. Chiba, and H. Koura, *J. Nucl. Sci. Technol.*, **43**, 1 (2006).
- [11] P. A. Moldauer, *Nucl. Phys. A*, **344**, 185 (1980).
- [12] T. Kawano and P. Talou, *Nuclear Data Sheets*, **118**, 183 (2014).
- [13] T. Kawano, P. Talou, and H. A. Weidenmüller, *Phys. Rev. C*, **92**, 044617 (2015).
- [14] C. Kalbach, *Phys. Rev. C*, **33**, 818 (1986).
- [15] A. J. Koning and M.C. Duijvestijn, *Nucl. Phys. A*, **744**, 15 (2004).
- [16] D. G. Madland and J. R. Nix, *Nuc. Sci. Eng.*, **81**, 213 (1982).
- [17] L. Bonneau, T. Kawano, T. Watanabe, and S. Chiba, *Phys. Rev. C*, **75**, 054618 (2007).
- [18] P. Möller, J. R. Nix, W. D. Myer, and W.J. Swiatecki, *At. Data and Nucl. Data Tables*, **59**, 185 (1995).
- [19] P. Möller, A. J. Sierk, T. Ichikawa, and H. Sagawa, *At. Data and Nucl. Data Tables*, **109**, 1 (2016).
- [20] T. Kawano and D. A. Brown, *J. Nucl. Sci. Technol.*, **52**, 274 (2015).
- [21] T. Kawano, T. Sanami, M. Baba, and H. Nakashima, *J. Nucl. Sci. Technol.*, **36**, 256 (1999).
- [22] C. A. Engelbrecht and Hans A. Weidenmüller, *Phys. Rev. C*, **8**, 859 (1973).